THE ASTROPHYSICAL JOURNAL, 262:358–368, 1982 November 1

CONSISTENCY OF THE MIXING LENGTH THEORY

D. NARASIMHA AND H. M. ANTIA
Tata Institute of Fundamental Research
Received 1982 January 27; accepted 1982 May 10

ABSTRACT

The structure of the solar convection zone calculated according to the mixing length theory is found to be consistent with the transport of convective flux by a linear superposition of statistically independent unstable convective modes, provided the effects of turbulent conductivity and viscosity are taken into account. The resultant vertical velocity is in reasonable agreement with observed granular velocity in the atmosphere, but the horizontal velocity turns out to be too large for low l modes.

Subject headings: convection — stars: interiors — Sun: interior

I. INTRODUCTION

The mixing length theory is extensively used in constructing stellar convection zone models. However, the question whether these models are consistent with models incorporating convective dynamics is not yet fully settled. Hart (1973) has convincingly demonstrated that no linear superposition of inviscid adiabatic modes can represent even approximately the convective heat flux of a stellar envelope. This is a consequence of all the modes having a sharp peak in the strongly superadiabatic layer near the top of the convection zone. Hart therefore concluded that convection predicted by the mixing length theory cannot be consistently represented as a combination of statistically independent inviscid adiabatic modes. To resolve this difficulty he has suggested the construction of a model using an iterative scheme such that the linear modes derived from it are consistent with the convective heat transfer assumed in the model. This approach may be used only if the amplitude of each mode can be computed independently. Bogart, Gierasch, and Macauslan (1980) have tried to follow this approach by including the effect of radiative damping in the calculation of linear modes. They have treated radiative dissipation in the optically thin approximation, and have demonstrated that it is possible to construct solar models such that the linear modes are consistent with the assumed convective flux. Unfortunately it turns out that these models are quite different from the currently accepted solar models. Thus it seems unlikely that such a self-consistent solar model will be able to explain the well known features of the Sun. Another difficulty with this approach is that there is no really satisfactory method for computing the amplitudes of each mode. Bogart *et al.* have argued that the amplitude will be limited by the Kelvin-Helmholtz instability, and, assuming the growth rate for this instability to be of the order of velocity shear, they have computed the amplitude of the convective modes.

Hart (1973) has also speculated on yet another alternative to resolve the difficulty by appealing to the non-adiabatic effects which are known to be very important in determining the nature of convective modes. Ever since Skumanich (1955) demonstrated that for a strictly adiabatic polytropic atmosphere the growth rate of convective modes increases monotonically with wavenumber, attention was focused on radiative effects as the probable mechanism to get a preferred length scale. The works of Böhm (1963) and Spiegel (1964) have clearly established the importance of radiative damping, although as far as the solar model is concerned Böhm (1963) failed to get any maximum in the growth rate as a function of the wavenumber. Antia, Chitre, and Pandey (1981, hereafter Paper I) and Narasimha, Pandey, and Chitre (1980) have emphasized the role of turbulent viscosity and conductivity in producing the length and time scales in accordance with observations for granulation and supergranulation, as well as the 5 minute oscillations, with the adoption of the currently accepted solar model (Antia, Chitre, and Narasimha 1982, hereafter Paper II). With this viewpoint we now proceed to examine Hart's problem by including turbulent viscosity and conductivity. We find that it is possible to construct a linear superposition of convective modes which reproduces convective flux in the solar convection zone reasonably well. It may not therefore be necessary to modify the mixing length theory to achieve self-consistency. We also calculate the velocity profile obtained by the linear superposition of these modes and compare it with observations.

II. MATHEMATICAL FORMULATION

a) *Basic Equations*

We shall adopt the usual hydrodynamical equations for the conservation of mass, momentum, and energy as being applicable to a viscous, thermally conducting fluid. These equations in the dyadic notation take the following form:

Mass conservation:

$$\frac{\partial \rho}{\partial t} + \nabla \cdot (\rho \boldsymbol{v}) = 0 \; ; \tag{2.1}$$

momentum conservation:

$$\rho \frac{\partial \boldsymbol{v}}{\partial t} + \rho(\boldsymbol{v} \cdot \nabla)\boldsymbol{v} = \rho \boldsymbol{g} - \nabla P - \tfrac{2}{3}\mu \nabla(\nabla \cdot \boldsymbol{v}) - \tfrac{2}{3}(\nabla \cdot \boldsymbol{v})\nabla \mu + \nabla \cdot [\mu(\nabla \boldsymbol{v} + \boldsymbol{v}\nabla)] \; ; \tag{2.2}$$

energy conservation:

$$\rho T\left(\frac{\partial s}{\partial t} + \boldsymbol{v} \cdot \nabla s\right) = -\nabla \cdot \boldsymbol{F} + \Phi \, , \tag{2.3}$$

where the rate of viscous dissipation

$$\Phi = \tfrac{1}{2}\mu(\nabla \boldsymbol{v} + \boldsymbol{v}\nabla) \cdot (\nabla \boldsymbol{v} + \boldsymbol{v}\nabla) - \tfrac{2}{3}\mu(\nabla \cdot \boldsymbol{v})^2 \, . \tag{2.4}$$

Here μ is the coefficient of dynamic viscosity, C_p the specific heat at constant pressure, s the specific entropy, $\nabla_{\rm ad}$ the logarithmic adiabatic gradient $(\partial \ln T/\partial \ln P)_{\rm ad}$, and F the total heat flux which is the sum of the radiative flux, F^R, and the convective flux, F^C. These equations must be supplemented by the equation of state. For this purpose we treat the medium as a perfect gas undergoing ionization, and we also include contribution due to radiation pressure (cf. Cox and Giuli 1968). We have adopted the same chemical composition as used by Spruit (1977). The radiative flux is computed in the Eddington approximation (Unno and Spiegel 1966) to get

$$\boldsymbol{F}^R = -\frac{4}{3\kappa\rho}\nabla J \, , \tag{2.5}$$

where

$$J = \sigma T^4 - \frac{\nabla \cdot \boldsymbol{F}^R}{4\kappa\rho} \tag{2.6}$$

is the intensity of radiation, σ the Stefan–Boltzmann constant, and κ the Rosseland mean opacity, which is computed from the opacity tables of Cox and Stewart (1970). In order to compute the convective flux, we adopt the standard mixing length formalism and write

$$\boldsymbol{F}^C = -K_t\left(\nabla T - \nabla_{\rm ad}\frac{T}{P}\nabla P\right) , \tag{2.7}$$

with the coefficient of turbulent heat conductivity taken to be of the form

$$K_t = \alpha \rho C_p W L \, . \tag{2.8}$$

In this expression α is the efficiency factor of order unity, L is the mixing length, and W the mean convective velocity given by

$$W = \left[\beta \frac{g}{H_p} Q L^2(\nabla - \nabla_{\rm ad})\right]^{1/2} . \tag{2.9}$$

Here β is a factor of order unity, H_p the pressure scale height, and $Q = -(T/\rho)(\partial\rho/\partial T)_P$ takes into account the change in mean molecular weight due to ionization. The molecular viscosity is negligible compared to the turbulent viscosity, and hence it is not considered here. For the turbulent dynamic viscosity we adopt the expression

$$\mu_t = P_t \alpha \rho W L \, , \tag{2.10}$$

where the turbulent Prandtl number P_t is treated as a free parameter; its value is selected to get the best possible agreement with observations.

We shall adopt the spherical geometry, and because of spherical symmetry in the equilibrium model the eigenfunctions for any scalar physical quantity in the perturbed state can be expressed as

$$f(r, \theta, \phi, t) = f_0(r) + f_1(r) Y_l^m(\theta, \phi) e^{\omega t} \, , \tag{2.11}$$

where the subscripts 0 and 1 respectively refer to the unperturbed and perturbed quantities, (r, θ, ϕ) are spherical polar coordinates with the radial coordinate r measured from the center of the Sun, $Y_l^m(\theta, \phi)$ are the spherical harmonics, and ω the growth rate. However, the velocity and flux perturbations will have the following form:

$$\boldsymbol{v}(r, \theta, \phi) = \left[v_r(r), v_h(r)\frac{\partial}{\partial\theta}, v_h(r)\frac{1}{\sin\theta}\frac{\partial}{\partial\phi}\right] Y_l^m(\theta, \phi) , \quad (2.12)$$

$$\boldsymbol{F}_1(r, \theta, \phi) = \left[F_r(r), F_h(r)\frac{\partial}{\partial\theta}, F_h(r)\frac{1}{\sin\theta}\frac{\partial}{\partial\phi}\right] Y_l^m(\theta, \phi) . \quad (2.13)$$

We linearize the basic equations by neglecting the higher order terms in perturbed quantities to get the following system of equations, with z measured downward from the level of optical depth unity:

$$\frac{dv_r}{dz} = \left(\frac{2}{r} - \frac{1}{H_\rho}\right)v_r - \frac{l(l+1)}{r} v_h + \frac{\omega}{\rho_0}\rho_1 , \quad (2.14)$$

$$-\frac{4\mu_{t0}}{r}\frac{dv_r}{dz} + \frac{d\mathscr{P}_r}{dz} = \left(\omega\rho_0 + \frac{4\mu_{t0}}{r^2}\right)v_r - \frac{2\mu_{t0}}{r^2} l(l+1)v_h - \frac{l(l+1)}{r}\mathscr{P}_h + g\rho_1 , \quad (2.15)$$

$$\mu_{t0}\frac{dv_h}{dz} = \frac{\mu_{t0}}{r} v_r - \frac{\mu_{t0}}{r} v_h + \mathscr{P}_h , \quad (2.16)$$

$$\frac{2\mu_{t0}}{r}\frac{dv_r}{dz} + \frac{d\mathscr{P}_h}{dz} = -\frac{2\mu_{t0}}{r^2} v_r + \left[\omega\rho_0 + \frac{2l(l+1)}{r^2}\mu_{t0} - \frac{2\mu_{t0}}{r^2}\right]v_h + \frac{3}{r}\mathscr{P}_h + \frac{1}{r}\mathscr{P}_r , \quad (2.17)$$

$$\frac{3K_{t0}T_0}{2C_{p0}}\frac{ds_1}{dz} = -F_0^C\left(\frac{\rho_1}{\rho_0} + \frac{T_1}{T_0} + \frac{1}{2}\frac{Q_1}{Q_0} - \frac{1}{2}\frac{C_{p1}}{C_{p0}}\right) + F_r^C , \quad (2.18)$$

$$\frac{4}{3\kappa_0\rho_0}\frac{dJ_1}{dz} = F_0^R\left(\frac{\kappa_1}{\kappa_0} + \frac{\rho_1}{\rho_0}\right) + F_r^R , \quad (2.19)$$

$$\frac{dF_r^R}{dz} = 4\kappa_0\rho_0\left[(J_0 - \sigma T_0^4)\left(\frac{\kappa_1}{\kappa_0} + \frac{\rho_1}{\rho_0}\right) - 4\sigma T_0^3 T_1\right] + \left[4\kappa_0\rho_0 + \frac{l(l+1)}{r^2}\frac{4}{3\kappa_0\rho_0}\right]J_1 + \frac{2}{r}F_r^R , \quad (2.20)$$

$$\frac{dF_r^R}{dz} + \frac{dF_r^C}{dz} = -\rho_0 T_0\frac{C_{p0}}{H_p}(\nabla - \nabla_{\rm ad})v_r + \left[\omega\rho_0 T_0 + \frac{l(l+1)}{r^2}\frac{K_{t0}T_0}{C_{p0}}\right]s_1 + \frac{l(l+1)}{r^2}\frac{4}{3\kappa_0\rho_0}J_1 + \frac{2}{r}F_r^R + \frac{2}{r}F_r^C , \quad (2.21)$$

$$\tfrac{4}{3}\mu_{t0}\left(\frac{3}{r} - \frac{1}{H_\rho}\right)v_r - 2\mu_{t0}\frac{l(l+1)}{r}v_h + \left(\tfrac{4}{3}\mu_{t0}\frac{\omega}{\rho_0}\right)\rho_1 + P_1 - \mathscr{P}_r = 0 . \quad (2.22)$$

In these equations, H_ρ is the density scale height, $\mathscr{P}_r$ and $\mathscr{P}_h$ are the negative of rr and $r\theta$ (or $r\phi$) components of the viscous stress tensor, and

$$F_0^R = \frac{16\sigma T_0^3}{3\kappa_0\rho_0}\frac{dT_0}{dz} \quad (2.23)$$

is the radiative flux in the unperturbed state. The perturbations to various physical quantities like κ, P, T, C_p, Q which are treated as functions of ρ and s can be expressed in the form:

$$f_1 = \left(\frac{\partial f}{\partial\rho}\right)_s\rho_1 + \left(\frac{\partial f}{\partial s}\right)_\rho s_1 , \quad (2.24)$$

where f can be any one of these quantities.

This system of equations constitutes a set of eight first order differential equations along with one auxiliary equation. Outside the convection zone $\mu_{t0} \equiv 0$ and $K_{t0} \equiv 0$ and hence the equations will simplify to a system of four first order differential equations.

b) Equilibrium Solar Model

For the present work we have adopted model A of Paper II which is characterized by the following choice of mixing length parameters:

$$\alpha = \tfrac{1}{4} , \quad \beta = \tfrac{1}{8} , \quad L = z + 459 \text{ km} .$$

We have considered the region outside the convection zone as inviscid. However, to allow for the overshoot of motion from subphotospheric layer into the bounding atmospheric region we have chosen the upper boundary between viscous and inviscid layers to be a little (264 km) above the actual convection zone boundary. We have verified that our results are not sensitive to the location of this boundary. As in Paper II we use the Kolmogoroff spectrum to estimate the coefficient of viscosity in the atmosphere.

c) Boundary and Connection Conditions

The equations governing the perturbed quantities form a set of eight first order differential equations in the central region (convection zone), while in the upper atmosphere as well as below the convection zone which are assumed to be inviscid the order of the governing equations reduces to four. Thus we need two boundary conditions at each boundary with six connection conditions at the boundary between the viscous and the inviscid regions.

We have adopted free boundary conditions at both the boundaries where the Lagrangian pressure perturbation is assumed to vanish, i.e.,

$$\delta P = 0 . \tag{2.25}$$

In addition, the thermal condition requiring the radiation not to come into the layer from infinity is imposed at the upper boundary, i.e.,

$$\delta(F/J) = 0 . \tag{2.26}$$

At the lower boundary we demand the vanishing of Lagrangian perturbation of flux: i.e.,

$$\delta F = 0 . \tag{2.27}$$

When we linearize the above three equations, we get

$$P_1 - g\rho_0 v_r/\omega = 0 , \tag{2.28}$$

$$\left[\frac{2}{r} + \frac{4\kappa_0 \rho_0 (J_0 - \sigma T_0{}^4)}{F_0{}^R} - \frac{3\kappa_0 \rho_0}{4J_0} F_0{}^R\right]\frac{v_r}{\omega} + \frac{J_1}{J_0} - \frac{F_r{}^R}{F_0{}^R} = 0 \tag{2.29}$$

at the upper boundary, and

$$P_1 - g\rho_0 v_r/\omega = 0 , \tag{2.30}$$

$$\frac{F_r{}^R}{F_0{}^R} - \frac{2}{r}\frac{v_r}{\omega} = 0 , \tag{2.31}$$

at the lower boundary.

At both the boundaries between the viscous and the inviscid layers we have imposed the following six conditions which can be obtained from the governing equations.

$$[\mathscr{P}_h] = 0 , \quad [\mathscr{P}_r] = 0 ,$$
$$[v_r] = 0 , \quad [F_r] = 0 ,$$
$$[s_1] = 0 , \quad [J_1] = 0 .$$

where the square brackets denote the jump across the boundary in the corresponding quantity.

The system of equations along with the boundary and connection conditions form a generalized eigenvalue problem where the eigenvalues and the associated eigenfunctions are to be determined for a specified value of the horizontal harmonic number l. We have solved the system numerically by a finite-difference scheme with explicit calculation of the first order correction (Antia 1979) as described in Paper I.

d) Consistency Requirement

As mentioned in the earlier section, the governing equations are solved for a specified value of l to get the growth rate ω and the eigenfunctions for the perturbed quantities. From these eigenfunctions one can caculate the energy flux transmitted by convection, for any given mode, by using the expression (cf. Bogart, Gierasch, and Macauslan 1980)

$$F_{l,n}(r) = \rho_0 v_r(T_0 s_1 + P_1/\rho_0) . \tag{2.32}$$

Note that here the eigenfunctions v_r, P_1, and s_1 are arbitrary to the extent of a constant multiple. To fix some normalization we choose this multiplicative constant such that the maximum of the convective flux $F_{l,n}(r)$ over the convection zone equals the actual convective flux $F_0{}^C(r)$ in the solar model at that point. If the model flux can indeed be represented as a linear superposition of statistically independent linear modes, then

$$\sum_{l,n} (a_{l,n})^2 F_{l,n}(r) = F_0{}^C(r) . \tag{2.33}$$

Here $a_{l,n}$ are real constants which fix the amplitudes of corresponding modes in the solar envelope. It should be noted that the summation extends over all the modes for which the growth rate ω is positive. Thus if we can find a set of real constants $a_{l,n}$ such that this equation is satisfied for all values of r inside the convection zone, then we would conclude that the mixing length theory is self-consistent.

III. NUMERICAL RESULTS

We have solved the system of equations governing viscous nonadiabatic convective modes to obtain the growth rate for a specified value of the horizontal harmonic number l. We get a series of eigenvalues ω for each value of l. These modes are characterized by the number of modes in the eigenfunction for radial velocity. We refer to the highest eigenvalue, the fundamental mode, as C1-mode and the successive harmonics by C2, C3, ... As in Paper II we select the value of Prandtl number P_t so as to get the best possible agreement with observations regarding length and time scales of granulation and supergranulation. This yields a value of $\frac{1}{3}$ for P_t which we have adopted in the present calculations.

In this work we shall be concerned with only those convective modes which have a positive growth rate. As noted in Paper I, only a finite number of modes have a positive growth rate. For $l \gtrsim 4000$ all the modes are found to be stable, while for lower values of l the fundamental (C1) mode is unstable. In addition, for $100 \lesssim l \lesssim 700$ the first harmonic (C2 mode) also turns out to be unstable, while the higher harmonics are always stable. Thus, unlike Hart's, our choice of modes is very limited. The properties of a sample of modes in this range are summarized in Table 1, which lists the growth rate and horizontal wavelength $\lambda = 2\pi R_\odot[l(l+1)]^{-1/2}$ for various modes. Figure 1 shows the convective flux as calculated by the mixing length theory as well as the convective flux carried by individual modes ($F_{l,n}$) for a few of the C1 modes. As mentioned earlier, the eigenfunctions are normalized such that the maximum of $F_{l,n}$ equals the total convective flux at that point. It can be easily seen that the different modes have maxima in $F_{l,n}$ at different depths and the maxima for values of l ranging between 6 and 2048 span almost the entire convection zone. Similarly, Figure 2 shows the convective flux carried by C2 modes along with the total flux as given by the mixing length model. Again it can be seen that the maxima of $F_{l,n}$ occur at different depths for different values of l. For these modes the flux becomes negative at certain depths; however, the negative

TABLE 1

CONVECTIVE MODES IN THE SOLAR ENVELOPE MODEL

Mode	l	Wavelength (km)	Growth Rate (s^{-1})	Weight Factor $(a_{l,n})^2$ (a)	(b)
C1	2	1,800,000	2.28(−7)	0.49	0.28
C1	3	1,270,000	3.92(−7)	...	0.25
C1	4	983,000	5.73(−7)	0.38	0.23
C1	6	678,000	9.66(−7)	...	0.16
C1	8	518,000	1.38(−6)	0.24	0.14
C1	12	352,000	2.26(−6)	...	0.12
C1	16	266,000	3.21(−6)	0.35	0.12
C1	24	179,000	5.28(−6)	...	0.15
C1	32	135,000	7.58(−6)	0.46	0.16
C1	48	90,600	1.28(−5)	...	0.17
C1	64	68,100	1.91(−5)	0.30	0.18
C1	96	45,600	3.60(−5)	...	0.19
C1	128	34,200	6.15(−5)	0.078	0.20
C1	192	22,800	1.44(−4)	...	0.22
C1	256	17,100	2.60(−4)	0.93	0.21
C1	384	11,400	5.37(−4)	...	0.16
C1	512	8580	8.24(−4)	0.0003	0.12
C1	768	5720	1.33(−3)	...	0.09
C1	1024	4290	1.71(−3)	0.0005	0.08
C1	1536	2860	2.10(−3)	...	0.08
C1	2048	2150	2.07(−3)	0.002	0.07
C1	3072	1430	1.19(−3)	0.49	0.05
C1	3548	1230	4.73(−4)	...	0.03
C2	144	30,400	3.26(−6)	...	0.10
C2	192	22,800	9.86(−6)	0.26	0.15
C2	256	17,100	1.82(−5)	...	0.18
C2	320	13,700	2.50(−5)	0.41	0.14
C2	384	11,400	2.99(−5)	...	0.10
C2	512	8580	3.20(−5)	0.08	0.07
C2	640	6860	2.18(−5)	...	0.03

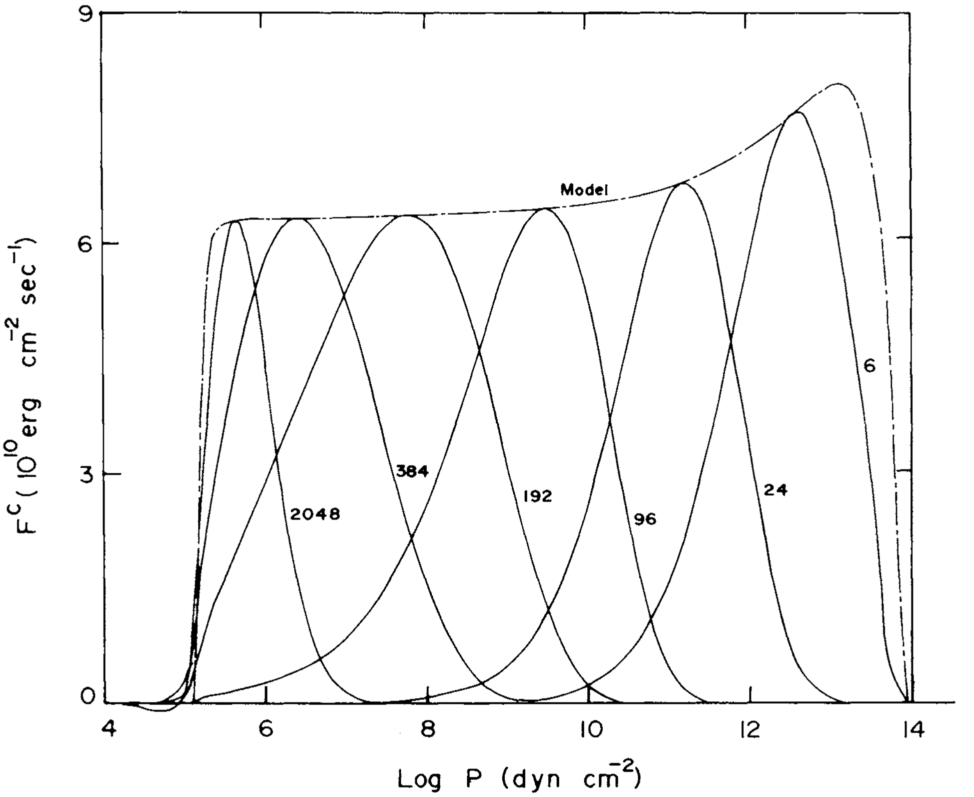

FIG. 1.—The convective flux transported by individual C1 modes is plotted against the logarithm of pressure for $l = 6$, 24, 96, 192, 384, and 2048. The curves are labeled by the value of l. The dot-dashed curve shows the convective flux as given by the mixing length model.

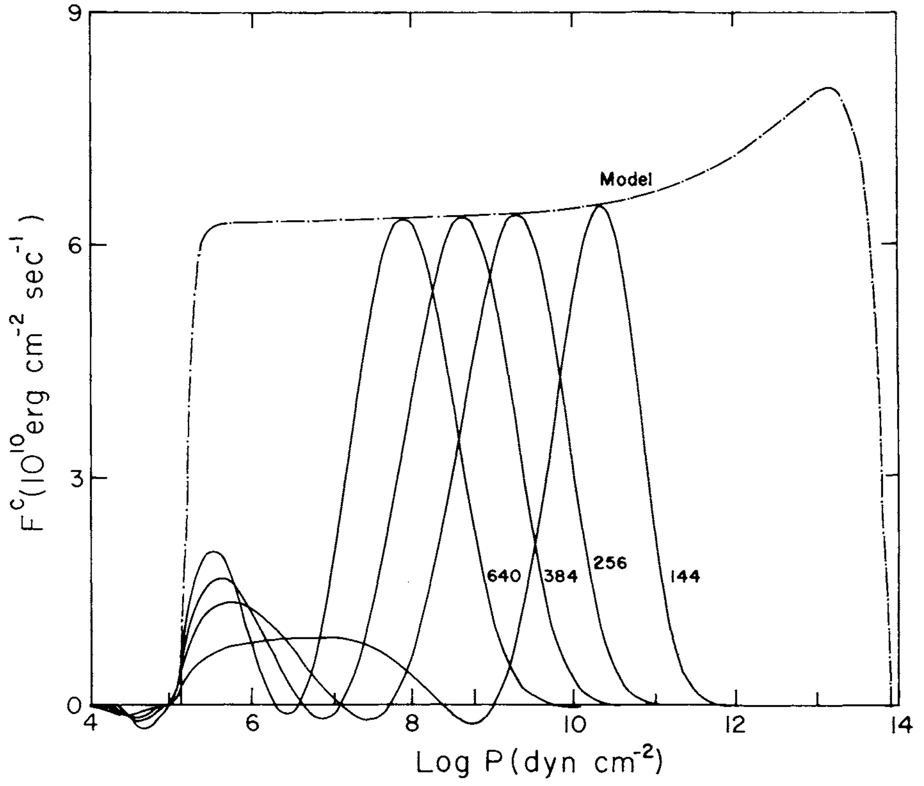

FIG. 2.—The convective flux transported by individual C2 modes is plotted against the logarithm of pressure for $l = 144$, 256, 384, and 640. The curves are labeled by the value of l. The dot dashed curve shows the convective flux as given by the mixing length model.

value of flux is very small. This is due to the fact that nodes of v_r, P_1, and s_1 do not coincide. It is clear from these figures that a suitable linear superposition of these modes should be able to reproduce the convective flux as predicted by the mixing length theory.

We have adopted two approaches to get a fit by linear superposition of modes with the model convective flux. In the first procedure we select a sample of 15 modes and attempt a least squares fit to get the weights $(a_{l,n})^2$ which are listed in column (5) of Table 1, and the curve (*b*) of Figure 3 displays the total flux profile obtained by using these weights. It can be seen that this total flux fits the mixing length value [shown by curve (*a*)] fairly well over the entire convection zone. Further, due to overshoot of convective modes into the atmosphere above the convection zone, the calculated flux does not vanish immediately outside the convection zone, but it is very small. It may be noted that in this fit the weights $(a_{l,n})^2$ are not a smooth function of *l*, probably because of numerical limitations in minimizing a function of 15 variables. Hence in our second approach we tried to get a fit in which the weights are smooth functions of *l*, and using 30 modes listed in Table 1 we get another fit the weights for which are listed in the last column of Table 1, with the total flux so obtained displayed by curve (*c*) of Figure 3. It can be seen that this fit is not as good as the first one and the calculated total flux oscillates about the model value. We believe that it should be possible to get a better fit in which the weights are a smooth function of *l*. In all our following work we have used the second fit because it has the weights which are smooth functions of *l*. Irrespective of the choice of the fit, it is clear from our results that a suitable superposition of statistically independent unstable convective modes can reproduce the radial dependence of the convective flux predicted by the mixing length theory, and hence the representations of the solar convection zone as a superposition of unstable linear modes is consistent with the mixing length theory. It may be noted that oscillatory modes will also transport some flux in the convection zone. We have tried to estimate this flux to find that if the amplitude of oscillatory modes is selected such that the velocity amplitude has a reasonable value in the atmosphere, then the convective flux carried by these modes comes out to be very small. We have neglected the contribution due to the oscillatory modes throughout the present work.

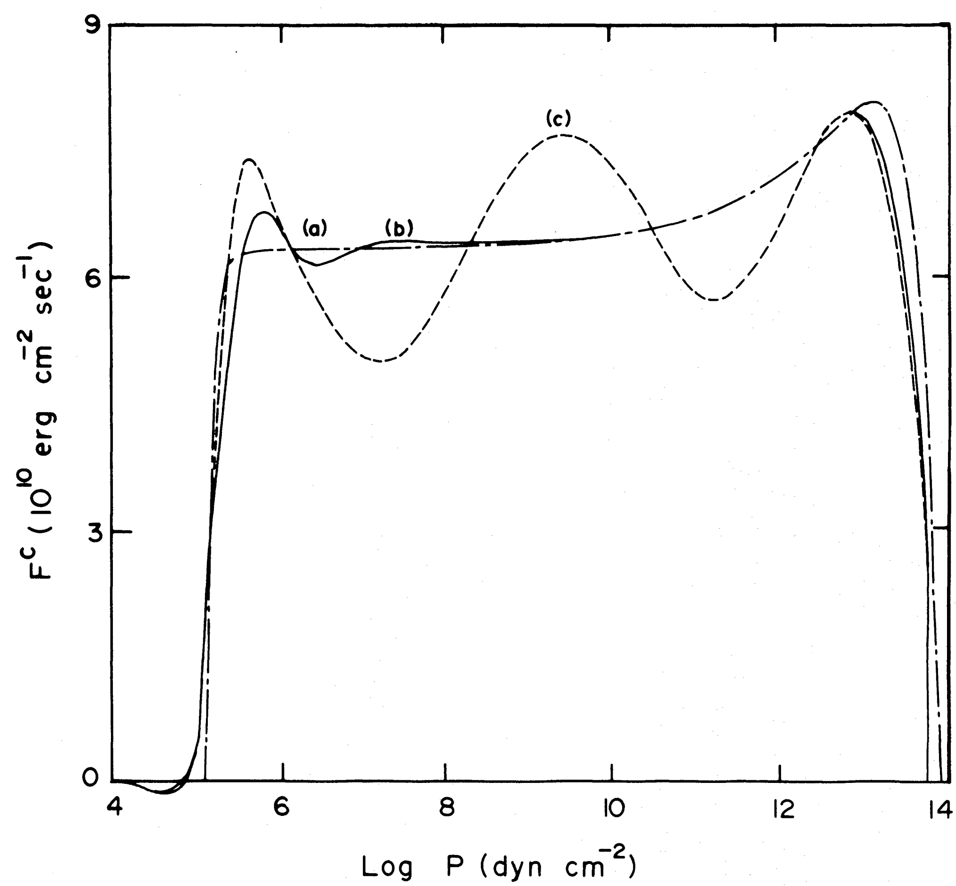

FIG. 3.—The total convective flux is plotted against the logarithm of pressure. (*a*) *Dot-dashed line*, value predicted by the mixing length model; (*b*) (*continuous line*) *and* (*c*) (*dashed line*) are the two fits obtained by the linear superposition of convective modes.

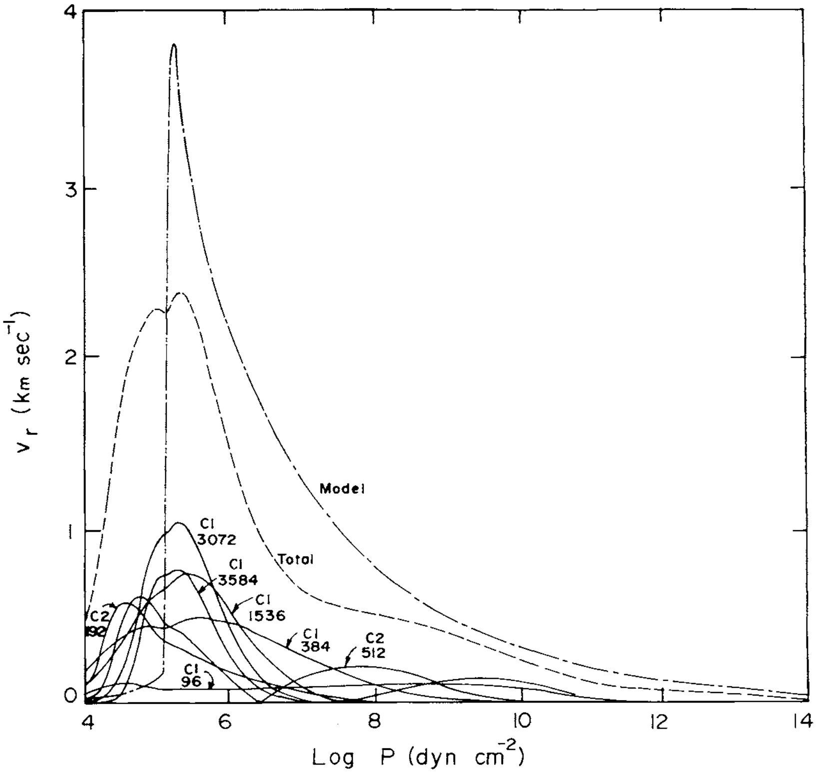

FIG. 4.—The contributions to the vertical velocity v_r by individual modes is plotted against the logarithm of pressure, for C1 modes with $l = 96$, 384, 1536, 3072, 3584 and C2 modes with $l = 192$ and 512. The contribution due to lower-l C1 modes is too small and is not shown. The curves are labeled by the values of l and the mode identification. The dashed curve shows the total vertical velocity contributed by superposition of all modes, while the dot-dashed curve shows the rms velocity yielded by the mixing length theory.

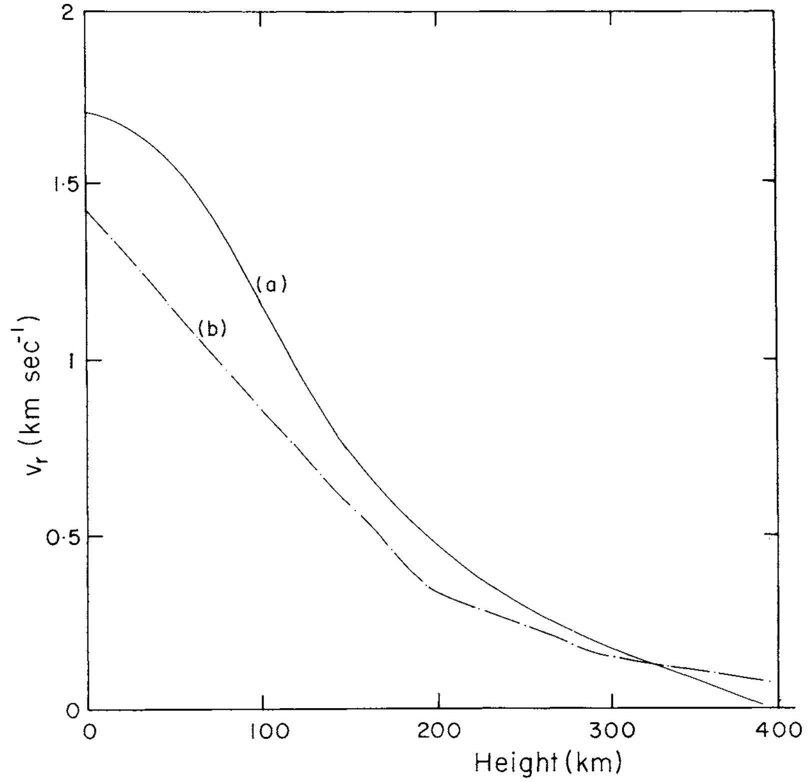

FIG. 5.—The continuous line shows the vertical velocity v_r contributed by modes with $l \gtrsim 1100$ plotted against height, while dot-dashed line shows the granular vertical velocity as given by Keil (1980).

We fix the amplitudes of various modes in solar convection zone by fitting the flux and in this manner remove the uncertainty of a constant multiple in the eigenfunction. Using these weights, we compute the velocity profile for various modes as well as the total velocity obtained by linear superposition. The results are displayed in Figures 4, 5, 6, and 7. The radial component of velocity for a sample of modes, as well as the total radial velocity obtained by superposition of all modes, is shown in Figure 4. Also shown is the rms velocity as predicted by the mixing length theory. It can be seen that the vertical velocity near the top of the convection zone is mainly contributed by the higher l ($\gtrsim 1000$) C1 modes and the C2 modes, while the small-l C1 modes make hardly any contribution to the vertical velocity. This is consistent with our interpretation (cf. Paper I) of granulation as C1 modes for higher l and supergranulation as C2 modes for $l \approx 400$. To compare the calculated profile with the observed value, we display in Figure 5 [curve (a)] the total vertical velocity contributed by modes with $l \gtrsim 1100$ ($\lambda \lesssim 4000$ km) which is compared with the empirical velocity profile [curve (b)] given by Keil (1980). It can be seen that the agreement is reasonable. The vertical velocity which is of the order of 1.8 km s^{-1} at the top of the convection zone falls off very rapidly with height and is only about 0.3 km s^{-1} at a height of 300 km above the level $\tau = 1$.

The horizontal component of velocity $v_H = [l(l+1)]^{1/2} v_h$ is shown in Figure 6 for a sample of modes. It can be seen that for low l the horizontal velocity increases steeply in the atmosphere. This is probably due to the sharp decrease in the density above the convection zone. The horizontal velocity comes out to be too large (~ 10 km s^{-1}) for the C2 modes, which is an order of magnitude larger than the observed values for supergranulation. However for high-l C1 modes it has a reasonable value of a few km s^{-1}, which is consistent with granular velocities. Figure 7 [curve (a)] displays the calculated profile for granular contribution to the horizontal velocity which can be compared with curve (b) showing the observed profile due to Keil and Canfield (1978). It can be seen that the agreement is not particularly good, which may be due to the incorrect boundary conditions or due to our neglect of turbulent pressure which will be important in the region around the top of the convection zone. As noted in Paper I, the boundary conditions do not affect the eigenvalues appreciably, but nevertheless the eigenfunctions in the atmospheric region close to the upper boundary may be quite sensitive to boundary conditions. We have

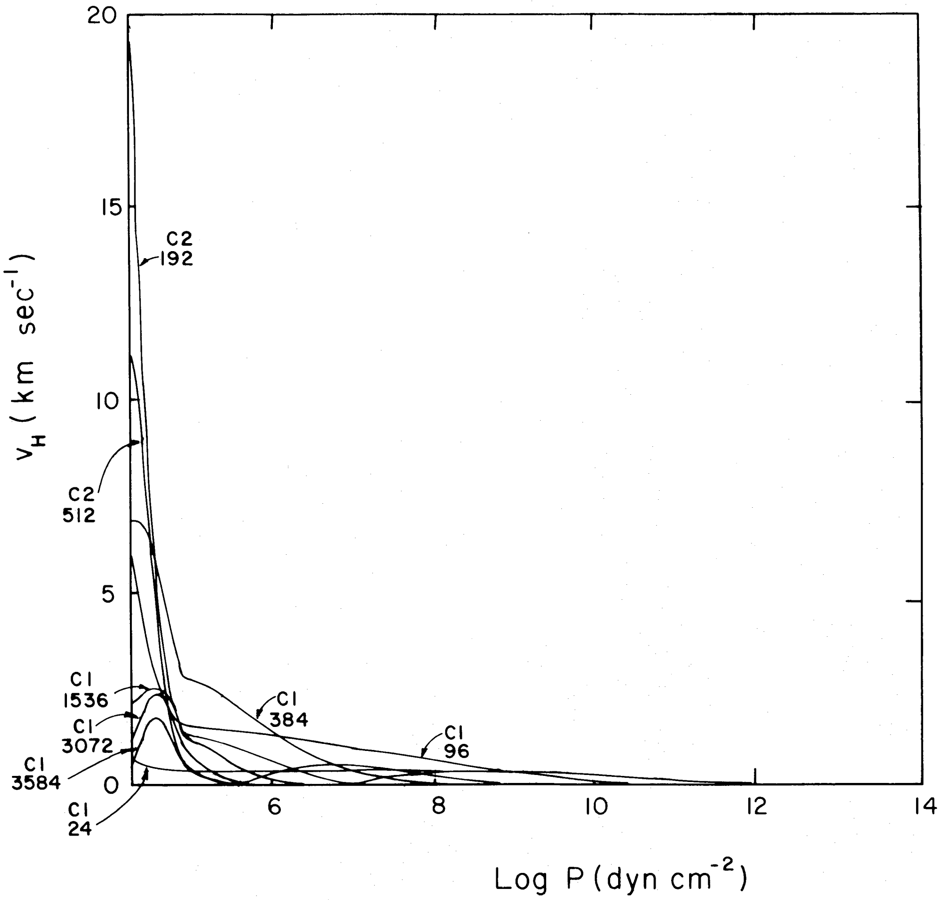

FIG. 6.—The horizontal velocity v_H contributed by individual modes is plotted against the logarithm of pressure, for C1-modes with l = 24, 96, 384, 1536, 3072, 3584; and C2 modes with l = 192 and 512. The curves are labeled by the values of l and mode identification.

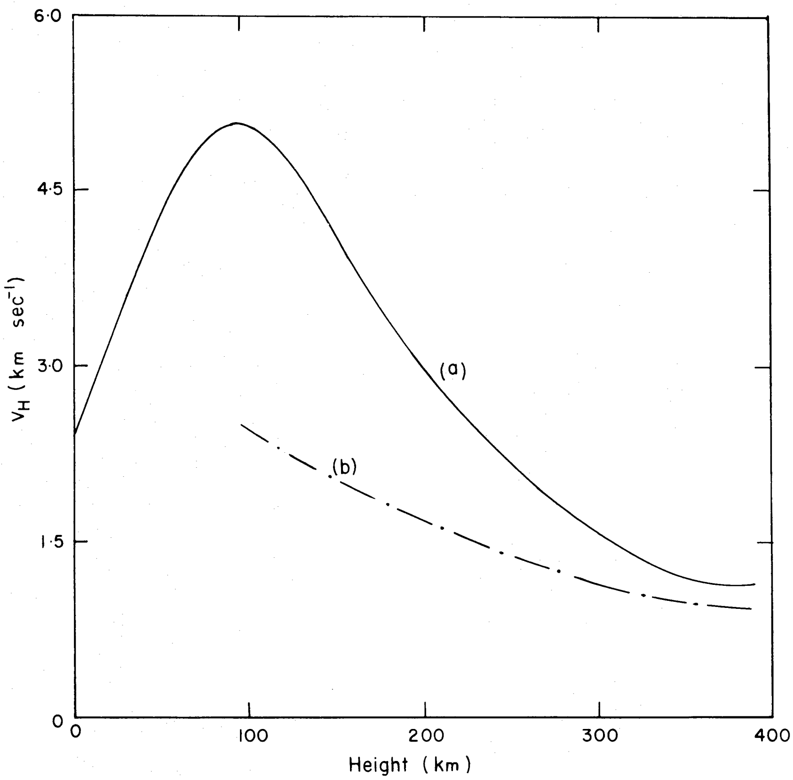

FIG. 7.—The continuous line shows the horizontal velocity v_H contributed by modes with $l \gtrsim 1100$ plotted against height, while the dot-dashed line shows the granular horizontal velocity as observed by Keil and Canfield (1978).

repeated the calculations with different boundary conditions as well as by shifting the boundary between the viscous and inviscid layers. We find that the horizontal velocity eigenfunctions in the atmospheric region do depend to some extent on the position of boundary between viscous and inviscid layers, but nevertheless the high value of horizontal velocity seems to persist.

We have also attempted to calculate the temperature fluctuations obtained by a superposition of various modes, and it comes out to be of the order of 500 K near the top of convection zone, which accords reasonably with observations (Keil and Canfield 1978).

IV. SUMMARY AND CONCLUSIONS

Our results clearly indicate that once the effects of turbulent conductivity and viscosity are included it is possible to get a linear superposition of statistically independent unstable convective modes which reproduces the convective flux as predicted by the mixing length theory over the entire convection zone. Thus the representation of the solar convection zone as a superposition of unstable linear modes is shown to be consistent with the mixing length theory. The failure of Hart (1973) and Bogart, Gierasch, and Macauslan (1980) to find consistency may be attributed to their neglect of dissipative effects which significantly modify the eigenvalues and eigenfunctions of these modes. Further, our work shows that it is not necessary to modify the mixing length theory as suggested by Bogart, Gierasch, and Macauslan (1980). It becomes somewhat difficult to calculate the solar convection zone model based on their suggestion, and in any case the model so obtained does not resemble the Sun in many of its well known properties. It is therefore encouraging to find that the standard solar model itself yields linear convective modes which are consistent with the mixing length theory in its usual form. Although we have not tested the consistency of mixing length models for other stars, we believe that even for these models the linear convective modes will be consistent with the standard mixing length theory.

It would, of course, be interesting to estimate the amplitude of these modes from a consideration of nonlinear processes, since that will enable us to predict the amplitudes without fitting the flux. These amplitudes can then be used to calculate the total flux for comparison with the model value. Further, we have neglected the effects of rotation and turbulent pressure in our calculation. The rotation is expected to affect the very low l modes, while the turbulent pressure will influence the eigenfunctions in regions around the top of the convection zone.

It is a pleasure to thank Professor S. M. Chitre for valuable discussions.

REFERENCES

Antia, H. M. 1979, *J. Comp. Phys.*, **30**, 283.
Antia, H. M., Chitre, S. M., and Narasimha, D. 1982, *Solar Phys.*, in press (Paper II).
Antia, H. M., Chitre, S. M., and Pandey, S. K. 1981, *Solar Phys.*, **70**, 67 (Paper I).
Bogart, R. S., Gierasch, P. J., and Macauslan, J. M. 1980, *Ap. J.*, **236**, 285.
Böhm, K.-H. 1963, *Ap. J.*, **137**, 881.
Cox, A. N., and Stewart, J. N. 1970, *Ap. J. Suppl.*, **19**, 243.
Cox, J. P., and Giuli, R. T. 1968, *Principles of Stellar Structure* (New York: Gordon & Breach).
Hart, M. H. 1973, *Ap. J.*, **184**, 587.
Keil, S. L. 1980, *Ap. J.*, **237**, 1024.
Keil, S. L., and Canfield, R. C. 1978, *Astr. Ap.*, **70**, 169.
Narasimha, D., Pandey, S. K., and Chitre, S. M. 1980, *J. Ap. Astr.*, **1**, 165.
Skumanich, A. 1955, *Ap. J.*, **121**, 408.
Spiegel, E. A. 1964, *Ap. J.*, **139**, 959.
Spruit, H. C. 1977, Ph.D. thesis, Utrecht.
Unno, W., and Spiegel, E. A. 1966, *Pub. Astr. Soc. Japan*, **18**, 85.

H. M. ANTIA and D. NARASIMHA: Theoretical Astrophysics Group, Tata Institute of Fundamental Research, Homi Bhabha Road, Bombay 400 055, India